ACS EARTH AND SPACE CHEMISTRY

Article

Cite This: ACS Earth Space Chem. 2019, 3, 1237−1247

http://pubs.acs.org/journal/aesccq

Emission and Evolution of Submicron Organic Aerosol in Smoke from Wildfires in the Western United States

Lauren A. Garofalo,[†] Matson A. Pothier,[†] Ezra J. T. Levin,[‡] Teresa Campos,[§] Sonia M. Kreidenweis,[‡] and Delphine K. Farmer*[,†]

[†]Department of Chemistry, Colorado State University, Fort Collins, Colorado 80523, United States

[‡]Department of Atmospheric Science, Colorado State University, Fort Collins, Colorado 80521, United States

[§]National Center of Atmospheric Research, Boulder, Colorado 80307, United States

Supporting Information

ABSTRACT: Despite increasing incidence of wildfires in the United States, wildfire smoke is poorly characterized, with little known about particle composition and emission rates. Chemistry in transported plumes confounds interpretation of ground and aircraft data, but near-field observations can potentially disentangle the effects of oxidation and dilution on aerosol mass and chemical composition. We report the organic aerosol (OA) emission ratios from aircraft observations near the fire source for the 20 wildfires sampled during the Western Wildfire Experiment: Cloud Chemistry, Aerosol Absorption, and Nitrogen (WE-CAN) study of summer 2018. We observe no changes in submicron nonrefractory OA mass concentration, relative to CO which accounts for simple dilution, between 0.5 and up to 8 h of aging. However, static OA excess mixing ratios hide shifts in the aerosol chemical composition that suggest near-balanced, simultaneous oxidation-driven condensation and dilution-driven evaporation. Specifically, we observe significant increases in the extent of oxidation, evident by an increase in oxidation marker f_{44} and loss of the biomass burning marker f_{60}, as the smoke ages through chemistry and dilution. We discuss the competing effects of oxidative chemistry and dilution-driven evaporation on the evolution of the chemical composition of aerosols in wildfire smoke over time.

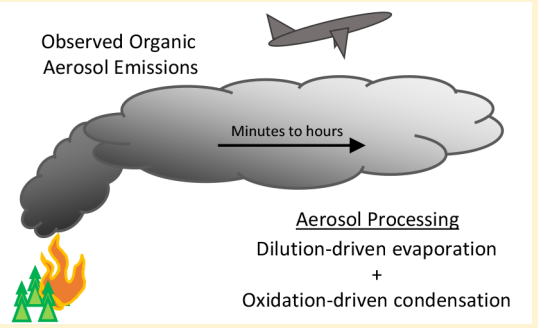

KEYWORDS: *atmospheric chemistry, biomass burning, organic aerosol, aerosol mass spectrometry, wildfire, Western United States*

1. INTRODUCTION

The number and intensity of wildfires in the western United States is increasing,[1] and the relative impact of emissions from wildfires on regional and global atmospheric composition is becoming more significant. Over the past three decades, $PM_{2.5}$ has generally decreased across the country, likely due to successful regulation of primary and secondary sources of particulate matter, except for regions that experience wildfires, specifically the mountain west.[2] Fire seasons are starting earlier and ending later due to changes in snowpack, precipitation, and temperature attributed at least in part to climate change.[3,4] Wildfires emit a variety of gases and particles that have major implications for air quality and climate. Aerosols have a profound impact on air quality for both human health and visibility,[5,6] and there is some evidence that aged aerosols have even higher toxicity than fresh aerosol.[7] Additionally, optical properties of aerosols, linked to chemical composition, can contribute to either a cooling or warming direct effect on the radiative balance of the planet, and can act as cloud condensation nuclei, contributing to an indirect effect on climate. However, wildfire impacts on aerosol concentrations, and thus air quality and climate, are challenging to model due to the lack of observational constraints on emissions as well as a lack of understanding of how aerosol changes as it ages. To better understand wildfire smoke chemistry in the western United States, we measured submicron nonrefractory organic aerosol (OA) emissions, chemical composition, and evolution in smoke from wildfires in the near-field (i.e., where smoke is less than 2 h old) and mid-field (i.e., where the smoke is less than 8 h old).

Two aspects of organic aerosol emissions from wildfires are particularly poorly understood: the variability in emissions during the course of a single burn and that between different burns of different fuels or environmental conditions, and the impact of chemistry on those emissions as they are transported in the atmosphere. Previously reported emission ratios (ERs) for OA from fires vary over orders of magnitude; the emission ratios, or mass concentration of OA relative to the coemitted CO ($ER_{OA} = \Delta OA/\Delta CO$, where Δ indicates enhancement above background levels) at or near the source, estimated from

Special Issue: New Advances in Organic Aerosol Chemistry

Received: May 1, 2019
Revised: June 11, 2019
Accepted: June 12, 2019
Published: June 12, 2019

DOI: 10.1021/acsearthspacechem.9b00125
ACS Earth Space Chem. 2019, 3, 1237−1247

aircraft measurements ranges from 0.02 to 0.55 μg m^{-3} ppbv^{-1} for wildfires under different conditions and regions.[8−14] Emission ratios from prescribed burns of coastal plains in South Carolina and mixed conifer in California vary less; e.g., May and co-workers[15,16] report emission ratios ranging from 0.04 to 0.11 μg m^{-3} ppbv^{-1}, but this consistency is likely due to the controlled burn conditions, such as fire temperature, fire stage, and fuel type. Despite this variation, these prescribed fires may not be representative of naturally occurring wildfires, which typically burn at hotter temperatures with more flaming combustion. Laboratory studies report fire-averaged OA emission ratios ranging from 0.02 to 1.76 μg m^{-3} ppbv^{-1} across fuel types and fire conditions.[16,17] For example, fire-averaged OA ERs for laboratory lodgepole pine burns ranged from 0.69 to 1.43 μg m^{-3} ppbv^{-1} for the same burn conditions and ERs for ponderosa pine burns ranged from 1.31 to 1.76 μg m^{-3} ppbv^{-1}.[16] In addition to these fire-averaged emissions ratios, Jolleys et al.[17] report an increase in "instantaneous" ER from 0.31 to 1.59 μg m^{-3} ppbv^{-1} during a single burn of ponderosa pine needles that was not observed in another burn of the same fuel despite nearly identical conditions (i.e., mass and moisture content of fuel, burn time). These differences are attributed to combustion efficiency and the timing of the transition between flaming and smoldering phases, with the smoldering phase generally producing more OA. Despite this illustrative example and a general link between smoldering and enhanced OA ERs, however, this study found that there was not a strong, consistent relationship between combustion efficiency and OA ERs across many fuel types.[17] A more recent study of laboratory burns showed a strong inverse logarithmic relationship between emission factor (ratio of species-of-interest emission to fuel mass, in contrast to the emissions ratio) for organic carbon (μg C m^{-3}) and modified combustion efficiency.[18] This further indicates that a smoldering fire will produce more OA than a flaming fire.

Rapid chemical evolution of smoke between initial emission and subsequent observation may also contribute to the large range in observed emission ratios of wildfire. As emissions are transported away from the source, photochemical oxidation by ozone (O_3) or OH radicals may produce secondary organic aerosol (SOA) from species with different volatility than primary organic aerosol (POA).[19] Additionally, condensation of organic molecules initially emitted in the gas phase at the hot ignition temperatures that subsequently cool and condense on aerosol surfaces can also contribute to SOA. This condensation would result in a net increase in OA mass concentration, relative to CO, as the plume moves downwind. In contrast, dilution of cleaner background air into the smoke plume can lead to a decrease in organic aerosol mass, beyond what can be accounted for by the dilution factor, due to changes in gas-particle equilibrium.[20] Dilution impacts gas-particle partitioning of organic aerosol by shifting the equilibrium for semivolatile organic compounds from the particle phase to the gas phase, leading to enhanced evaporation at lower concentrations.[21] In smoke plumes, this dilution-driven evaporation should enhance partitioning from the particle to the gas phase downwind. Additionally, as dilution occurs at the edges of the plume, particles should partition more strongly to the gas phase at the edges relative to the center of the plume.[20,22,23] This dilution would result in a net decrease in OA mass concentration, relative to CO, as the plume moves downwind.

The relative balance of these two competing factors, oxidation chemistry followed by condensation, and evaporation of semivolatile components due to dilution, in aging plumes is under debate. In some smoke plumes, increases in the OA ER have been observed and interpreted as evidence of condensation and/or SOA formation.[9,11] However, other studies have observed slight decreases in OA ERs[13,24,25] or no change as the plume ages.[8,15,22,26] These fundamental differences in organic aerosol evolution in plumes do not follow clear patterns, and instead show ranges in behavior in the near-field. For example, in a smoke plume in the Yucatan, OA ERs increased by a factor of 2 in 1.5 h, attributed to SOA formation.[9] However, Akagi et al.[24] show that in a California chaparral smoke plume, OA ERs decreased during the first 1.5−2 h, followed by a period in which the observed emission ratio stabilized, or possibly even increased. Though complicated by urban anthropogenic sources, DeCarlo et al.[11] observed an increase in OA emissions ratio with plume age for one fire, but a decrease in another fire. Similarly, OA ERs from prescribed burns in South Carolina showed increased OA emission ratios with age for one fire, and no change with age for another.[15] Finally, a study of multiple smoke plumes in western Africa found no changes in OA mass.[8] The discrepancies in how OA ERs change over time could be due to an array of reasons, including differences in the smoke injection height (boundary layer versus free troposphere) and differences in background concentrations of diluting air. Plume OA concentration also likely plays a large role in the balance between OA evaporation and condensation. Akagi et al.[24] hypothesized that condensation in the more concentrated California smoke plume would have occurred faster than in the dilute Yucatan smoke plume, and was the primary process controlling OA ERs in the California smoke plume after 1.5−2 h. However, while some hypotheses exist, the lack of consensus on OA aging in smoke plumes is complicated by the limited numbers of observations in the near-field, challenging model development to parametrize emissions and predict OA concentrations downwind.

Regardless of whether a change in emission ratio is observed, the extent to which the OA in smoke plumes was oxidized increases with age.[8,11,22,23] This chemical evolution, even when accompanied by no OA mass change, indicates that chemical and physical processes are rapidly occurring in the smoke plume. Oxidation reactions can form more functionalized species that have lower volatilities, with each step in oxidation lowering volatility by an order of magnitude,[21] though these reactions can also lead to fragmentation and thus more volatile organic molecules. This chemical evolution and subsequent SOA growth increases the elemental ratio of oxygen to carbon (O:C) in OA,[27] and also the fractional component of OA attributed to the CO_2^+ ion (f_{44}). Oxidation by OH is the likely culprit, thought to be produced in smoke plumes through the photolysis of formaldehyde, a primary emission from fires.[28] Levoglucosan is a common biomass burning marker and can be oxidized in the particle phase with an OH rate constant of 1.1 ($\pm$0.5) × 10^{-11} cm^3 molecule^{-1} s^{-1}, implying a lifetime of 1.1 days (assuming [OH] of 10^6 molecules cm^{-3}).[29] An aircraft study of smoke plumes inferred an in-plume average OH concentration of 5.27 ($\pm$0.97) × 10^6 molecules cm^{-3}.[24] However, not all studies are consistent, and some models of smoke plumes suggest depleted OH in the plume compared to background levels due to the high OH reactivity of gas-phase emissions.[28] Additionally, there is substantial evidence that

DOI: 10.1021/acsearthspacechem.9b00125
ACS Earth Space Chem. 2019, 3, 1237−1247

ozone can form rapidly inside the smoke plume from reaction of OH with emitted VOCs and NOx, which are emitted from fires in large quantities, although this ozone may be depleted as the smoke plume ages.[30] Regardless of the mechanism, previous studies of OA aging in wildfire smoke plumes have consistently observed marked increases in oxidation, identified by elemental O:C or fractional component f_{44}.

To improve our understanding of the emission and evolution of organic aerosol in wildfire smoke, we measured smoke from 20 wildfires in the Western United States at the source and downwind. We report 15 emission ratios of OA from near-passes of fires and investigate the chemical evolution of the organic aerosol as the plumes aged through chemistry and dilution for 12 fires.

2. METHODS

2.1. Campaign. The Western Wildfire Experiment for Cloud Chemistry, Aerosol Absorption, and Nitrogen (WE-CAN) was a multiagency project to intensively characterize the emissions and evolution of those emissions from wildfires in the Western United States. WE-CAN took place during July - September of 2018 and used the NSF/NCAR C-130 aircraft to sample regional smoke and smoke emitted from specific wildfires in the western United States during 19 flights. Sixteen research flights were operated from Boise, Idaho, and three educational flights from Broomfield, Colorado. The payload included a large suite of gas and particle instruments. (https://www.eol.ucar.edu/field_projects/we-can) Here, we will describe only those instruments used as part of this work.

2.2. Instrumentation. A high-resolution time-of-flight aerosol mass spectrometer (HR-AMS; Aerodyne Inc.) with a pressure controlled inlet[31,32] was used to detect submicron nonrefractory aerosol mass and composition. We operated the HR-AMS in V-mode (mass resolution ~2100 $m/\Delta m$) with 5 s time-resolution in mass spectrometry mode (2.5 s open and 2.5 s closed). The pressure controlled inlet maintained a constant lens pressure of 1.35 Torr and flow rate of 84.4 sccm. We used the High Resolution ToF-AMS Analysis Toolkit v1.20 (Aerodyne, Inc.) in Igor Pro (Wavemetics, Inc.) for postprocessing and analyzing the data. The high aerosol concentrations observed inside the smoke plumes necessitated several changes to the standard data-processing scheme. Specifically, rather than using a unit mass resolution (UMR) airbeam correction which is typically used to correct for small fluctuations in instrument signal, we implemented an airbeam correction using a high resolution peak[33] (Ar^+ at m/z 39.962) to avoid the overcorrection during high aerosol loadings due to interfering masses and subsequent underestimation of aerosol mass concentrations. (Supporting Information section 1, Figure S1). We also applied a time-dependent CO_2 correction using simultaneous observations of CO_2 mixing ratios to accurately account for the contribution of gas phase CO_2 to the CO_2^+ ion signal.

The number and mass concentrations of refractory black carbon (rBC) were measured by using a single particle soot photometer (SP2; Droplet Measurement Technologies).[34,35] An SP2 uses a 1064 nm Nd:YAG laser to heat absorbing material to its vaporization temperature and measures the resulting incandescence, which is proportional to the incandescing mass. The SP2 sample line was diluted with HEPA-filtered ambient air to prevent signal saturation during high aerosol loading periods.

Carbon monoxide (CO) was measured with two instruments: a quantum cascade laser instrument (CS-108 miniQCL, Aerodyne, Inc.)[36] and a cavity ring down spectrometer (G2401-m WS-CRD, Picarro). The CO-QCL had better precision than the CO-CRD (2σ = ±1 ppbv vs 50 ppbv), and the CO-QCL was used in all analyses presented herein excepting 13 Aug 2018 and 13 Sept 2018. The Picarro G2401-m WS-CRD also detected CO_2 (2σ = ± 0.1 ppmv).

We averaged all measured variables to the time base of the AMS sampling (5 s) to maintain high time resolution in the AMS data. Before averaging to the AMS time-base, the data were synchronized in time to account for variations in sample line length, flow rate, and instrument response rate.

2.3. Normalized Excess Mixing Ratio Calculations. The normalized excess mixing ratio (NEMR) is the ratio of enhancement above background of a species ($\Delta X = X - X_{bkg}$) to the enhancement above background for CO ($\Delta CO = CO - CO_{bkg}$), and accounts for simple dilution of clean air into the plume.

$$\mathrm{NEMR} = \frac{\Delta X}{\Delta CO} = \frac{X - X_{\mathrm{bkg}}}{\mathrm{CO} - \mathrm{CO}_{\mathrm{bkg}}} \quad (1)$$

For organic aerosol, the term "mixing ratio" is a misnomer since aerosol mass concentrations are generally reported in $\mu g\ sm^{-3}$, but for consistency, we will use that name and note that the units for NEMR of OA is $\mu g\ sm^{-3}\ ppb^{-1}$.[15] The NEMR is considered to be the emission ratio of the species if measured at the source, i.e., in the absence of any dilution effects or chemical changes. For species with lifetimes longer than the time period of interest, NEMR does not change as the plume is diluted into background air. Changes in NEMR as a function of plume age indicate net gain or loss of the species due to physical or chemical changes. However, as cautioned in Yokelson et al.,[37] simple mixing effects, especially in regions with variable backgrounds, may cause a change in NEMR that is not related to chemistry or physical changes. In this way, both the source variability and mixing effects may alter the NEMR, complicating the interpretation of the values. The NEMR also assumes no significant production of CO in the plume from oxidation, a reasonable assumption as CO has a lifetime in the troposphere of 2 months[38] with negligible chemical production.[39]

The NEMR can be estimated several ways:

(1) Slope method: The NEMR is calculated as the slope of the relationship between the species of interest and CO for which the background of the species of interest is zero or constant. The slope method removes the challenge of defining a background as the slope of the relationship is independent of intercepts. However, poor correlation between CO and the species of interest for reasons including discrepancies in instrument timing (e.g., if the time resolutions of the detection techniques are different) can introduce substantial uncertainty in the NEMR.

(2) Plume integration method with explicit background subtraction: The NEMR is calculated from the ratio of the background-subtracted integrated values across a plume. The challenge is determining the correct background. For laboratory studies of fuel burning, the backgrounds are taken as the concentrations measured prior to the start of the experiment. However, in aircraft-based studies of fire emissions, the background can vary throughout the length of

DOI: 10.1021/acsearthspacechem.9b00125
ACS Earth Space Chem. 2019, 3, 1237−1247

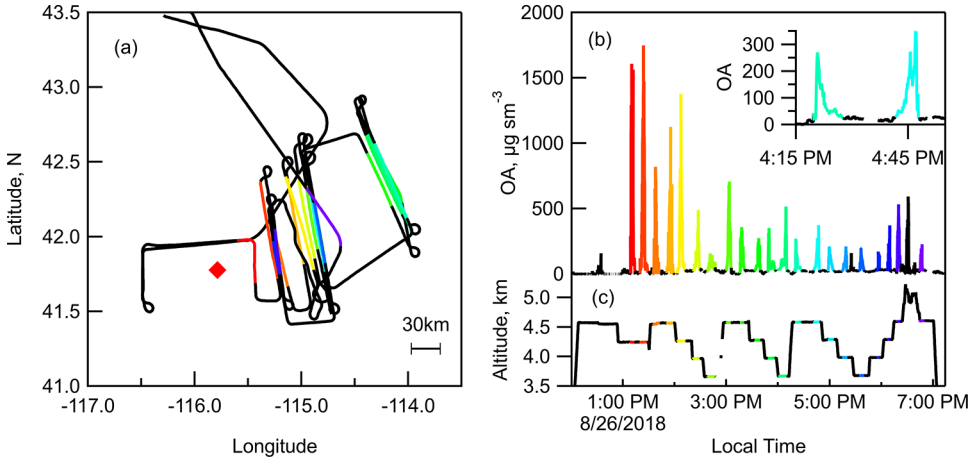

Figure 1. (a) Flight track for the South Sugarloaf fire (fire location marked with red diamond) for RF15, 26 Aug 2018. The time series of (b) organic aerosol (OA, μg sm^{-3}) and (c) altitude (km) versus local time shows the plume transects colored by time. The inset highlights the time series of OA for two transects, demonstrating differences in the shape of the plume and the OA concentration of background air on the two sides of the plume.

the plume and even can be different on each side of a plume cross section.

(2a) Upwind background: We first assume that the air upwind of the fire represents the background (upwind background). This would be appropriate when the upwind air and the edges of the plume are indeed free from influences of older smoke. However, new smoke from the fire of interest can dilute into already smoky air from other fires, and the air on the edges of the plume may be spatially heterogeneous, so that the background behind the fire fails to represent the background into which the plume is diluting. In some instances, one side of the plume can be diluted by cleaner background than the other.

(2b) Intertransect background: The background is estimated as the average of the 15 s immediately before and after each plume transect.

(2bi) Transect background: Each individual transect through the plume has its own background. This accounts for changing composition of the background air as the plume moves away from the fire, but ignores differences in background air between one side or the other of an individual plume.

(2bii) Fire-average background: In this approach, we average the transect backgrounds for each fire to provide a single background value for each smoke plume. This method is useful when the aircraft did not access the background air for at least 15 s before and after the plume-transect. This method ignores changing background composition downwind of a plume.

For OA NEMR, the slope method (1) and the plume-integration using an explicit background subtraction using the intertransect backgrounds (both transect and fire-average backgrounds: 2bi,ii) agree well. The plume-integration method using the upwind background (2a) underestimates NEMR relative to the other methods by 8−25% (Supporting Information section 2, Figure S2). The analyses below use the plume-integration method with explicit fire-averaged background.

2.4. Plume Age. We estimate the plume age as the haversine distance between the aircraft position and the burned area of a fire, estimated for the time that the aircraft sampled the fire by the U.S. Forest Service, divided by the average in-plume wind speed measured on the NCAR/NSF C-130 for a given fire, similar to analysis in other studies.[15,40] We assume that the plume rose above the burning location to the altitude at which we sampled the fire, and then was advected to the sampling location at a constant wind speed. Uncertainty in plume age from these assumptions is estimated to be 6−40% for different smoke plumes, with a mean uncertainty of 18%, based on the variance of windspeed for different passes through a single targeted smoke plume.

3. RESULTS AND DISCUSSION

3.1. Overview of Sampling. During WE-CAN, smoke plumes from 20 distinct fires were sampled 22 times using a pseudo-Lagrangian approach: after sampling background air behind the plume, the aircraft sampled the fire of interest close to the source, before transecting the plume perpendicular to the wind direction away from the fire. The Federal Aviation Administration (FAA) and air traffic control placed temporary flight restrictions on airspace above active fires, which determined the minimum distance to the fire and the altitude at which we sampled the plume.

Figure 1 shows an example flight path, altitude, and time series of organic aerosol measured by the HR-AMS for a flight on 26 August 2018. The target fire was the South Sugarloaf fire in Nevada (41.77N, 115.79W). The plume was transected near the source of the fire at three different altitudes before moving downwind; downwind transects were repeated at the same three altitudes. In this manner, we sampled the smoke at three different distances and three different altitudes before returning to the source of the fire and resampling the nearest transect. The closest transect was 30 km, and the farthest transect was 150 km away from the fire. The time series shows the number of plume transects. The OA concentration is at its maximum of 1700 μg sm^{-3} during the first set of passes nearest the plume. OA concentrations were lower during the second set of passes at the same location 5 h later, reaching only 500 μg sm^{-3}. OA concentrations decrease with distance from the fire due to dilution, reaching 270 μg sm^{-3}, or 6.5 times less, at 150 km. In this case, the South Sugarloaf smoke plume was diluted by background air that was heavily impacted by older smoke (days to weeks old) on the north side of the plume. This background smoke was ubiquitous in the western United States during late summer 2018 due to transport of smoke

DOI: 10.1021/acsearthspacechem.9b00125
ACS Earth Space Chem. 2019, 3, 1237−1247

from fires in California (e.g., the Mendocino complex) and British Columbia. The inset in Figure 1b highlights the asymmetry of the plume by showing two transects that were performed in opposite directions through the plume (i.e., the aircraft crossed the plume, performed a 180° turn, and crossed back through the plume again). This plume, in particular, had very different edges: one edge, the first side through the first transect, was sharp and diluted by relatively clean background air, while the second edge was more diffuse and diluted by already smoky air. On the second pass in the opposite direction, we observe the same structure: we entered the more diffuse side and exited the sharper side. The older smoke complicates the background calculation for NEMR, potentially affecting dilution and photon flux that occurs on the edges of the plume.

The analysis herein assumes that plumes maintained vertical homogeneity throughout the plume, and that in the pseudo-Lagrangian case studies, we sampled the plume at the same height. However, in reality, smoke plumes rise and disperse in three dimensions with complex dynamics.[41] The multiple altitudes sampled for the South Sugarloaf fire allows us to probe this effect in one fire. With the exception of a few vertical profiles done by vertical spirals, and flights with these different altitude legs, we are sampling a three-dimensional process in only two dimensions, so some differences between flights may be due to the fact that while we may be able to identify the center of the plume in horizontal space, we do not fully characterize the vertical structure of the plume.

3.2. Submicron Nonrefractory Aerosol Chemical Composition. The aerosol nonrefractory composition from the sampled fires was primarily organic (85−96%) with smaller contributions from nitrate, ammonium, sulfate, and chlorine (Figure 2), although we note that these components can be associated with organic aerosol (e.g., the nitrate signal includes contribution of organic nitrates, $RONO_2$, and the sulfate signal includes organic sulfate and sulfonic acid). Black carbon was a small component (<2%) of the submicron mass in the sampled plumes. Previous work has shown that aerosol from wildfires is almost entirely organic (>90%)[12,14] and that aerosol generated by laboratory burns of ponderosa and lodgepole pine are almost all organic aerosol (OA > 95%), while there are higher fractions of sulfate and rBC in fuels such as sagebrush and white and black spruce (OA < 50%).[16] Preliminary fuel inventory estimates for the South Sugarloaf fire indicate that the predominant ecosystems burned were low sagebrush steppe, black cottonwood−Douglas fir−quaking aspen riparian forest, so the chemical composition measured here is inconsistent with burns of these individual components. Additionally, the organic fraction measured in prescribed grass fires in South Carolina was ∼70% organic aerosol while montane fires showed that the fraction was 90% OA and 10% rBC with very little contribution from inorganic components.[16] The composition and evolution of the inorganic aerosol component from sampled wildfires will be discussed in a separate manuscript.

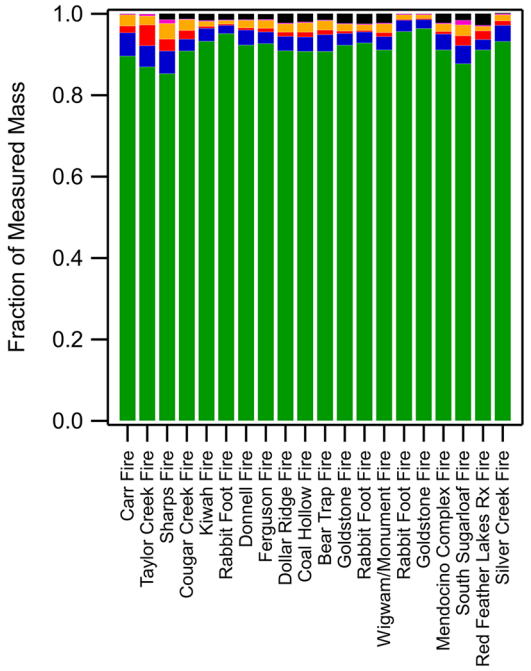

Figure 2. Fraction of measured mass for organic (green), inorganic (pink, chloride; red, sulfate; orange−ammonium; blue, nitrate) and black carbon (black) components of nonrefractory submicrometer aerosol averaged for all plume transects for each fire.

3.3. NEMR of Organic Aerosol. The NEMR of OA for all flights that sampled concentrated smoke attributed to a specific fire are shown as a function of plume age in Figure 3. As discussed in the Introduction, a change in NEMR signifies that chemical or physical processes beyond simple dilution have occurred as the plume ages. For the fires shown, the NEMR of OA remained unchanged as the aircraft sampled air downwind of the fires. On initial inspection, our observations indicate that there was no net loss or gain of OA through chemical or physical processes in the first 0.5−8 h of aging. This observation is consistent with results from some prescribed burns and wildfires,[8,15,22,26] but not consistent with either the previously observed increases in OA NEMR that were attributed to SOA formation,[9,11] or the slight decreases in

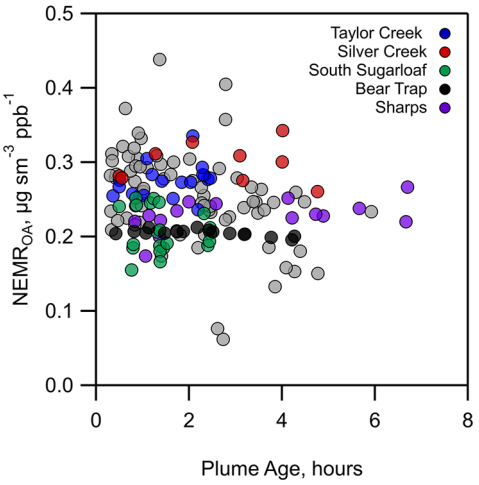

Figure 3. NEMR of OA, using background-subtracted plume-integrated OA and CO, as a function of physical plume age. Data from four fires that were particularly well sampled in a pseudo-Langrangian sense have been colored; these four fires were sampled across the plume perpendicular to the wind direction at multiple points downwind. These data highlight the apparent lack of change in the NEMR of OA with plume age.

DOI: 10.1021/acsearthspacechem.9b00125
ACS Earth Space Chem. 2019, 3, 1237−1247

OA NEMR attributed to strong evaporation of the organic aerosol.[13,24,25]

The lack of net change in OA mass in the plume relative to CO with distance from the fire is consistent with two opposing hypotheses: (1) that no chemistry or physics occurs on the observed time scales (transport of plumes for <8 h) or (2) that photochemistry occurs in the plume, but with no net effect on total organic aerosol mass. We explore these hypotheses below.

The analysis of plume-integrated NEMRs assumes that the smoke is well-mixed and that the aging clock starts when the plume begins horizontal transport at the altitude at which the smoke was sampled. However, smoke undergoing convection in the smoke plume could be from distinct regions of fire stage (i.e., flaming on the edges of the fire versus smoldering in the already burned center; plume both cools and dilutes during vertical convection). Also, once the smoke starts horizontal motion, there is real structure in the edges of the plumes; that is, filaments of clean air are imperfectly mixed with the plume air, creating areas of lower concentration within the plume boundaries (e.g., Figure S3).[41] These are accounted for by integration techniques and weighted averages, so that this clean air does not disproportionally affect the plume integrated or plume averaged values. However, dilution of the edges of these filaments may occur at different rates than in other parts of the plume.

3.4. Variability in Emission Ratios. The NEMR for the closest passes to the fire with ages between 20 min and 1 h were assumed to represent the ER for that species, relative to CO. The OA ERs are reported for sampled smoke plumes less than 1 h old and range from 0.18−0.30 μg sm^{-3} ppb^{-1} (Figure 4). While these OA emissions ratios are comparable to previous laboratory and aircraft studies,[16,17] we speculate that differences between laboratory-based studies and field burns are due to rapid chemical and physical changes, including repartitioning,[42] that occur in the near-field due to rapid cooling and dilution during vertical convection prior to sampling the fires.

The WE-CAN data set includes repeated measurement of emissions near the source for multiple fires, either hours or days apart. For example, the South Sugarloaf Fire was sampled near the source twice, separated by 5 h. The ER of OA decreased by 28% from the first pass to the second pass 5 h later; in contrast, the ER of rBC increased by 61%. These data are consistent with the fire shifting from the smoldering to flaming stage through the afternoon−highlighting the challenges of extrapolating observations of a single emissions measurement, or attributing observed emission ratios to a fire type. A previous study of smoke from western wildfires[14] reports NEMR of OA of 0.33 ± 0.098 μgm^{-3} ppbv^{-1} for plumes attributed to smoldering fires compared to 0.26 ± 0.098 μgm^{-3} ppbv^{-1} for plumes attributed to flaming fires from ground and aircraft-based measurements of smoke with transport times ranging from 1 to 40h. Fire behavior evolves with time, leading to changes in the emissions ratios.

As noted in the Introduction, the range of ΔOA/ΔCO values reported for wildfires ranges from 0.02 to 0.55 μg m^{-3} ppbv^{-1} across different regions.[8−13] Liu et al.[12] report ΔOA/ΔCO ratios of 0.28−0.39 μg m^{-3} ppb^{-1} for three fires in the western United States, which has remarkable agreement with the 15 OA emission ratios reported here. These ERs are more than two times greater than the emission ratios measured in prescribed burns, but can be lower than laboratory burns.

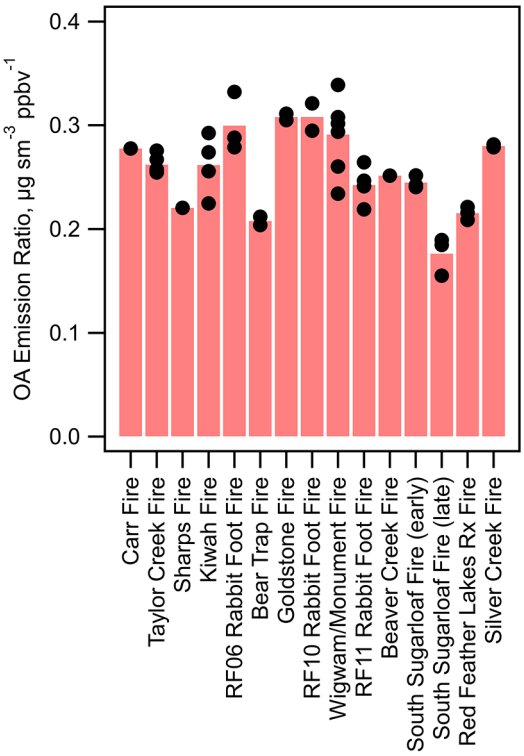

Figure 4. OA emission ratios are presented as an average (bars) and individual value for each plume transect (black circles) for each fire sampled at estimated tranport times of less than 1 h. For the South Sugarloaf fire, the two near-source passes are separated into "early" and "late" for the passes sampled 5 h apart.

3.5. Chemical Evolution of Organic Aerosol. The chemical components of OA elucidate the chemical and physical processes that are occurring in the aerosol as the plume evolves. While we did not observe changes in OA NEMRs as the smoke aged (up to 8 h), chemical markers did change dramatically with age. For this reason, the first hypothesis, that no physical or chemical changes beyond simple dilution are occurring in the OA in the first few hours of aging, can be eliminated, so we consider possible factors responsible for changes in chemistry, but not net mass, in OA. In particular, gases present in the smoke plume could be undergoing oxidation chemistry and subsequently condensing onto the particle phase. These gas phase precursors can be semivolatile components of POA that have evaporated, or direct gaseous emissions from the wildfire plume. Such oxidation chemistry enhances OA mass concentration. Multiphase chemistry in liquid aerosol could enhance downwind OA, as has been proposed for levoglucosan,[29] though plumes were generally dry during this study. However, to achieve no net change in OA beyond simple dilution, this SOA production must be balanced by a loss process. One likely loss process is dilution-driven evaporation in which simple dilution reduces OA concentration and pushes the gas-particle equilibrium to favor evaporation, which then decreases the OA mass concentration beyond that for simple dilution. A balance between oxidation-driven condensation and dilution-driven evaporation would result in no changes in OA NEMR, but marked changes in chemical composition. Here, we examine the evolution of two markers, f_{44} and f_{60}, as the smoke plume ages and is diluted by background air. The fractional ratio f_{44} is

DOI: 10.1021/acsearthspacechem.9b00125
ACS Earth Space Chem. 2019, 3, 1237−1247

the ratio of the integrated signal of the CO_2^+ ion (at m/z 43.990; calculated in high resolution) detected by the HR-AMS to the total OA signal and is well correlated with the elemental O:C ratio of the bulk OA;[43] f_{60} is the ratio of the integrated signal of $C_2H_4O_2^+$ (m/z 60.021) to total OA. The CO_2^+ signal represents fragments of acids or acid-derived species.[44] Primary organic aerosol from biomass burning is generally hydrocarbon-like, with low f_{44} and low O:C ratio.[27] f_{44} and O:C will increase if the bulk aerosol becomes more oxidized, and so f_{44} has been used as a tracer for SOA (and aged POA).[23,27] The $C_2H_4O_2^+$ signal in the AMS is considered to be predominately the result of fragments of levoglucosan and other anhydrous sugars produced by the pyrolysis of cellulose, and is thus an indicator of fresh biomass burning.[45−47] However, levoglucosan is semivolatile, and a substantial fraction of its mass can be lost due to dilution.[48,49] Levoglucosan can also be oxidized by OH via multiphase reactions in the aerosol liquid phase with uptake coefficients depending on relative humidity.[29,50] While levoglucosan oxidation marks a decrease in f_{60}, it does not necessarily translate to a net loss of organic mass from the aerosol, as products likely remain in the particle phase. To summarize, an increase in f_{44} with plume age will be driven by increased fractions of oxidized organic compounds, consistent with SOA formation and evaporation of more volatile compounds, while a decrease in f_{60} will be driven by oxidation and evaporation of semivolatile levoglucosan and other anhydrous sugars.

Figure 5 shows plume averages of f_{44} (a) and f_{60} (b) for each plume transect as a function of physical age. The plume transect nearest to the source is generally the one with the highest f_{60} and the lowest f_{44}. While the variability of f_{44} and f_{60} in the freshest emissions is quite large, the aging processing seems to be consistent across fires. Figure 5c shows the same data as f_{44} vs f_{60}; this data visualization was first discussed in Cubison et al.[23] for smoke aged for days or weeks, finding increased OA oxidation (f_{44}) with simultaneous loss of levoglucosan-like species (f_{60}) and that f_{60} is a persistent, but not inert, tracer of biomass burning aerosol on the time scale of days to weeks. In the 12 fires studied as pseudo-Lagrangian experiments during WE-CAN, as the smoke aged on the time scale of hours, the chemical composition generally increased in oxidation (f_{44} increased) and decreased in the anhydrous sugar fragments due to multiphase chemistry and/or dilution-driven evaporation (f_{60} decreased). This observed aging is consistent with other measurements of f_{44} and f_{60} from biomass burning aircraft-based studies.[22,23] Laboratory studies of aging of biomass burning emissions have shown that the rates at which f_{44} increases and f_{60} decreases can differ significantly across fuel type, and may be connected to the initial OA concentration.[33] Ahern et al.[19] shows that aging of biomass burning emissions by OH and O_3 in chamber experiments results in an increase in f_{44} and decrease in f_{60} in each oxidative scheme. However, in laboratory studies, the change in OA chemical composition is generally accompanied by an increase in OA NEMR, and the observed OA enhancement is attributed to condensational growth of the particles from less-volatile oxidized species. However, in our work, as in some previous field studies,[8,15,22,26] the lack of change in dilution-adjusted OA mass (i.e., NEMR) requires a balance between evaporation of the semivolatile species and condensation of the lower volatility species that results in a change in OA chemical composition, but no net change in OA mass concentration, corrected for dilution.

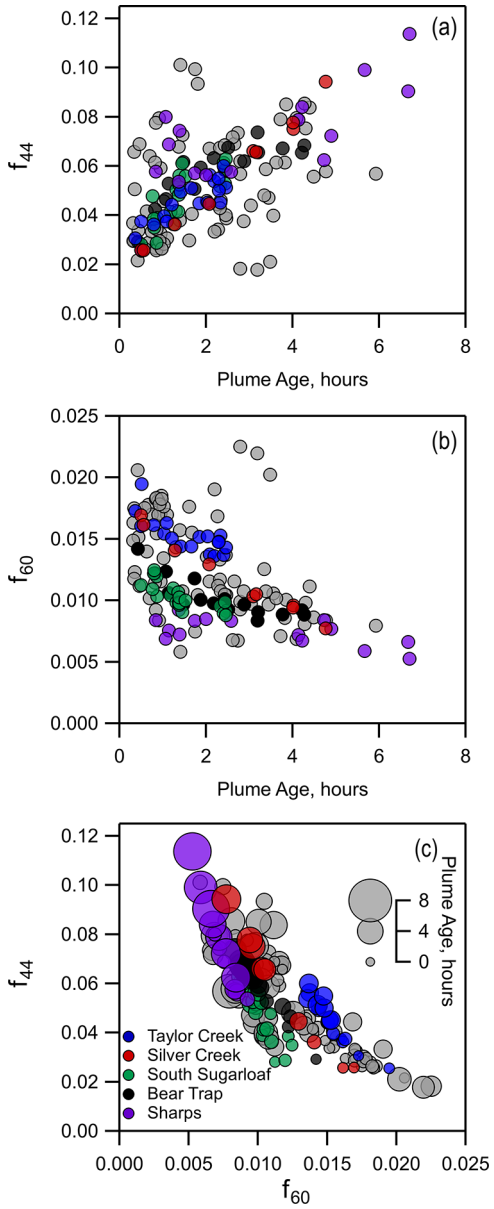

Figure 5. Fractional component f_{44} (a) increases and f_{60} (b) decreases as a function of plume mean age (all fires gray; four highlighted fires in color). As the plume ages, f_{44}, a proxy for oxidation, increases, and f_{60} decreases, indicating loss of levoglucosan. The simultaneous shift in fractional components is shown in (c).

3.6. Variation in Organic Aerosol Chemical Composition Across the Plume. Organic aerosol chemical composition changed during each transect through the cross section of the plume. For plumes that were sufficiently wide with diffuse edges (i.e., where the aircraft spent between 100 and 400 s in the plume during an individual transect), we observed clear differences in chemical composition between the center and edges of the plume. At typical ground speed of the NSF/NCAR C-130 aircraft through plumes of ~130 m s^{-1}, 100−400 s corresponds to approximately 13−52 km. The South Sugarloaf fire provides a particularly clear example of this change in OA chemical composition (Figure 6). The f_{44} ratios were smallest at the center of the plume, while the f_{60} ratios were the largest. The difference in f_{44} at the edges versus the center of a single plume transect were larger than the

DOI: 10.1021/acsearthspacechem.9b00125
ACS Earth Space Chem. 2019, 3, 1237−1247

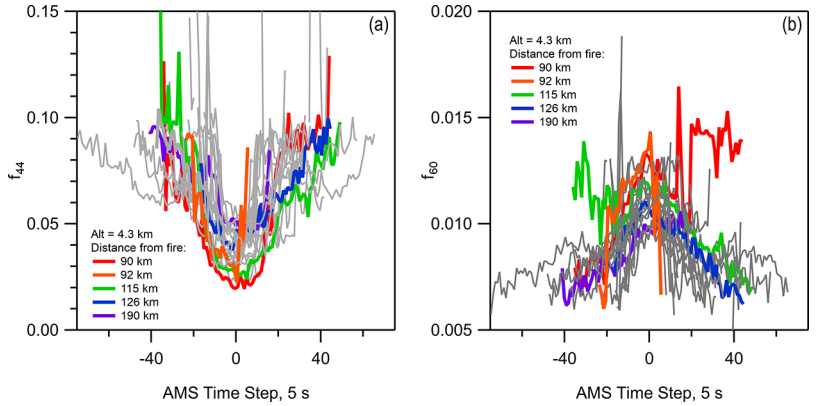

Figure 6. f_{44} (a) and f_{60} (b) versus AMS 5 s time step for 20 plume transects from the South Sugarloaf fire with plume transects from the same altitude highlighted in color. The plume transects have been aligned so that the middle of the plume, determined by a Gaussian fit of the OA versus time for a given plume transect, is at $t = 0$. The fractional component f_{44} at the center of the plume is lower than at the edges of the plume while f_{60} is generally higher at the center of plume. The variability within a single transect is larger than the differences between downwind transect-to-transect of the same plume in some cases.

transect-to-transect differences for this fire. For example, the transect-averaged f_{44} for the South Sugarloaf fire ranged between 0.025 and 0.060 (Figure 5a), while the change for some individual plume passes were much larger (0.02−0.12; Figure 6a). The plume edges likely experienced both more photochemistry, due to optically thinner aerosol loadings, and more dilution (and thus dilution-driven evaporation) than the center of the plume. The f_{44} at the center of the plume generally increased with distance from the fire source, similar to the analysis presented above derived from transect averages and consistent with condensation of more oxidized components. The suppressed f_{44} in the center relative to the edges could be consistent with either enhanced oxidation at the edge of the plume, or dilution-driven evaporation of less oxidized hydrocarbon-like material at the edges of the plumes that enhanced the fraction of less volatile oxidized organic components. Consistent with this hypothesis, the f_{60} ratios (Figure 6b) were largest in the center of the plume, which suggests that dilution-driven evaporation of the semivolatile levoglucosan was occurring more rapidly at the plume edges.

Downwind plume analysis showed no net enhancement of OA over time which suggests that sources and sinks of OA balance one another. However, these sources and sinks may not balance within the cross section of a plume. In the cross-plume transect, if only evaporation were occurring, we would expect f_{60} to be maximized, f_{44} to be minimized, and OA NEMR to be maximized at the center of the plume. Upon dispersion and dilution with cleaner air, evaporation of the semivolatile levoglucosan would reduce f_{60}; species with low volatility and high f_{44} would remain in the particle phase while other components of OA would evaporate, lowering f_{44}, and OA mass on the edges would be reduced beyond simple dilution due to this shift in gas-particle partitioning of volatile and semivolatile species to favor the gas phase. Conversely, if only oxidation were occurring, we would expect f_{60} to be maximized at the center, however with a smaller magnitude on the time scale of a few hours of aging because levoglucosan has a lifetime of 1.1 days against OH.[29] We would also expect f_{44} to be at a minimum at the center of the plume, and no change or a slight increase in NEMR through condensation of less volatile oxidation products. For the South Sugarloaf fire, we observed that f_{60} was at a maximum and f_{44} a minimum at the center of the plume. However, the NEMRs calculated from single data points are extremely sensitive to the background used, more so than for the plume-integrated NEMRs, so it is difficult to determine the shape of a cross-plume NEMR with a high degree of certainty.

This analysis assumes that the smoke throughout each plume transect represents the same emission (i.e., each cross section samples smoke emitted at the same time), and that smoke is well-mixed during turbulent vertical convection so that the smoke is uniform across the plume before it begins horizontal transport (i.e., the smoke at plume edges does not have a different fuel or fire temperature than the smoke at the center). Therefore, a plume-transect analysis may reduce the impact of potential fluctuations in fire emissions over time. The transect-averaged f_{44} and f_{60} are determined by weighted average using OA mass concentration rather than by arithmetic mean. In this way, the chemical composition of OA in the middle of the plume, where the majority of aerosol mass exists, is weighted more strongly compared to the edges. This weighted average more accurately reflects the bulk of the aerosol, however caution should be taken in transect-averaged or plume-integrated values since, in some cases as shown by the OA chemical composition, the edges and the center are very distinct due to differences in processing inside the dense dark center of the plume compared to the dilute lighter edges of the plume.

4. CONCLUSION

For the 20 wildfires sampled at the near-field during the WE-CAN campaign, we observed that the submicron aerosol was overwhelming organic (85−96%) and determined emission ratios between 0.18−0.30 μg sm^{-3} ppbv^{-1}, showing the relatively narrow range of ERs for organic aerosol from wildfires in the western U.S. For the 12 fires sampled via pseudo-Lagrangian methods, we consistently observed no increase in OA mass, once corrected for dilution, but did observe an increase in oxidation tracer f_{44} and a decrease in biomass burning tracer f_{60} with smoke age. The increased exposure to oxidants [OH and O_3] and clean air that drives gas-particle equilibrium resulted in the gain of more oxidized species, as evident by the increase in f_{44}, and the loss of the semivolatile tracers of biomass burning from levoglucosan and other anhydrous sugars, as evident by the decrease in the f_{60} fragment. While a combination of photooxidation and dilution-

DOI: 10.1021/acsearthspacechem.9b00125
ACS Earth Space Chem. 2019, 3, 1237−1247

driven evaporation effects may result in an increase in the oxidized organic portion of OA, the lack of net increase or decrease in OA mass indicates that there was a near-equal balance between evaporation and condensation in the near- and mid-field observed during these flights. The discrepancy between laboratory studies, which typically show an increase in OA mass with aging, and field measurements indicates that SOA formation is considerable in chamber studies, but its importance may be overestimated in smoke plumes if dilution-driven evaporation is not considered.

We observe that even if OA processing in smoke plumes does not change OA mass, corrected for simple dilution, the chemical composition of the OA does indeed change to an increased oxidation level with higher f_{44} and O:C. Previous work indicates that an increase in OA oxidation level, in general, is linked to increases in aerosol density,[51,52] hygroscopicity,[53] absorption,[54] and toxicity.[7] Therefore, while we show that OA mass does not change beyond simple dilution, changes in chemical composition with links to physical and optical properties could make the existing mass a more efficient cloud condensation nuclei or absorber, which has implications for the overall impact of aerosol emitted from wildfire on climate, air quality, and health.

■ ASSOCIATED CONTENT

Supporting Information

The Supporting Information is available free of charge on the ACS Publications website at DOI: 10.1021/acsearthspacechem.9b00125.

Summary of sampled fires, including flight dates, locations, and OA emission ratio; detailed description of HR-ToF-AMS data acquisition and processing; description of background calculations for NEMR; additional figures for cross-plume analysis (PDF)

■ AUTHOR INFORMATION

Corresponding Author

*E-mail: delphine.farmer@colostate.edu.

ORCID

Lauren A. Garofalo: 0000-0001-7593-2580

Delphine K. Farmer: 0000-0002-6470-9970

Notes

The authors declare no competing financial interest.

■ ACKNOWLEDGMENTS

This study was supported by NOAA Climate Program Office's Atmospheric Chemistry, Carbon Cycle, and Climate program (Grant NA17OAR4310010) and the National Science Foundation (Grant NSF-1650786) for WE-CAN. We would like to acknowledge operational, technical and scientific support provided by NCAR's Earth Observing Laboratory, sponsored by the National Science Foundation and all WE-CAN science teams. We thank Roger Ottmar for fire fuel and fire location information.

■ REFERENCES

(1) Dennison, P. E.; Brewer, S. C.; Arnold, J. D.; Moritz, M. A. Large wildfire trends in the western United States, 1984−2011. *Geophys. Res. Lett.* **2014**, *41* (8), 2928−2933.

(2) McClure, C. D.; Jaffe, D. A. US particulate matter air quality improves except in wildfire-prone areas. *Proc. Natl. Acad. Sci. U. S. A.* **2018**, *115* (31), 7901−7906.

(3) Jolly, W. M.; Cochrane, M. A.; Freeborn, P. H.; Holden, Z. A.; Brown, T. J.; Williamson, G. J.; Bowman, D. M. J. S. Climate-induced variations in global wildfire danger from 1979 to 2013. *Nat. Commun.* **2015**, *6*, 7537.

(4) Abatzoglou, J. T.; Williams, A. P. Impact of anthropogenic climate change on wildfire across western US forests. *Proc. Natl. Acad. Sci. U. S. A.* **2016**, *113* (42), 11770−11775.

(5) Liu, J. C.; Wilson, A.; Mickley, L. J.; Dominici, F.; Ebisu, K.; Wang, Y.; Sulprizio, M. P.; Peng, R. D.; Yue, X.; Son, J. Y.; Anderson, G. B.; Bell, M. L. Wildfire-specific fine particulate matter and risk of hospital admissions in urban and rural counties. *Epidemiology* **2017**, *28* (1), 77−85.

(6) Deflorio-Barker, S.; Crooks, J.; Reyes, J.; Rappold, A. G. Cardiopulmonary effects of fine particulate matter exposure among older adults, during wildfire and non-wildfire periods, in the United States 2008−2010. *Environ. Health Perspect.* **2019**, *127* (3), No. 037006.

(7) Chowdhury, P. H.; He, Q. F.; Male, T. L.; Brune, W. H.; Rudich, Y.; Pardo, M. Exposure of lung epithelial cells to photochemically aged secondary organic aerosol shows increased toxic effects. *Environ. Sci. Tech Let* **2018**, *5* (7), 424−430.

(8) Capes, G.; Johnson, B.; McFiggans, G.; Williams, P. I.; Haywood, J.; Coe, H. Aging of biomass burning aerosols over West Africa: Aircraft measurements of chemical composition, microphysical properties, and emission ratios. *J. Geophys Res-Atmos* **2008**, *113*, D00C15.

(9) Yokelson, R. J.; Crounse, J. D.; DeCarlo, P. F.; Karl, T.; Urbanski, S.; Atlas, E.; Campos, T.; Shinozuka, Y.; Kapustin, V.; Clarke, A. D.; Weinheimer, A.; Knapp, D. J.; Montzka, D. D.; Holloway, J.; Weibring, P.; Flocke, F.; Zheng, W.; Toohey, D.; Wennberg, P. O.; Wiedinmyer, C.; Mauldin, L.; Fried, A.; Richter, D.; Walega, J.; Jimenez, J. L.; Adachi, K.; Buseck, P. R.; Hall, S. R.; Shetter, R. Emissions from biomass burning in the Yucatan. *Atmos. Chem. Phys.* **2009**, *9* (15), 5785−5812.

(10) Hodgson, A. K.; Morgan, W. T.; O'Shea, S.; Bauguitte, S.; Allan, J. D.; Darbyshire, E.; Flynn, M. J.; Liu, D. T.; Lee, J.; Johnson, B.; Haywood, J. M.; Longo, K. M.; Artaxo, P. E.; Coe, H. Near-field emission profiling of tropical forest and Cerrado fires in Brazil during SAMBBA 2012. *Atmos Chem. Phys.* **2018**, *18* (8), 5619−5638.

(11) DeCarlo, P. F.; Dunlea, E. J.; Kimmel, J. R.; Aiken, A. C.; Sueper, D.; Crounse, J.; Wennberg, P. O.; Emmons, L.; Shinozuka, Y.; Clarke, A.; Zhou, J.; Tomlinson, J.; Collins, D. R.; Knapp, D.; Weinheimer, A. J.; Montzka, D. D.; Campos, T.; Jimenez, J. L. Fast airborne aerosol size and chemistry measurements above Mexico City and Central Mexico during the MILAGRO campaign. *Atmos. Chem. Phys.* **2008**, *8* (14), 4027−4048.

(12) Liu, X. X.; Huey, L. G.; Yokelson, R. J.; Selimovic, V.; Simpson, I. J.; Muller, M.; Jimenez, J. L.; Campuzano-Jost, P.; Beyersdorf, A. J.; Blake, D. R.; Butterfield, Z.; Choi, Y.; Crounse, J. D.; Day, D. A.; Diskin, G. S.; Dubey, M. K.; Fortner, E.; Hanisco, T. F.; Hu, W. W.; King, L. E.; Kleinman, L.; Meinardi, S.; Mikoviny, T.; Onasch, T. B.; Palm, B. B.; Peischl, J.; Pollack, I. B.; Ryerson, T. B.; Sachse, G. W.; Sedlacek, A. J.; Shilling, J. E.; Springston, S.; St Clair, J. M.; Tanner, D. J.; Teng, A. P.; Wennberg, P. O.; Wisthaler, A.; Wolfe, G. M. Airborne measurements of western US wildfire emissions: Comparison with prescribed burning and air quality implications. *J. Geophys Res-Atmos* **2017**, *122* (11), 6108−6129.

(13) Jolleys, M. D.; Coe, H.; McFiggans, G.; Capes, G.; Allan, J. D.; Crosier, J.; Williams, P. I.; Allen, G.; Bower, K. N.; Jimenez, J. L.; Russell, L. M.; Grutter, M.; Baumgardner, D. Characterizing the aging of biomass burning organic aerosol by use of mixing ratios: A meta-analysis of four regions. *Environ. Sci. Technol.* **2012**, *46* (24), 13093−13102.

(14) Collier, S.; Zhou, S.; Onasch, T. B.; Jaffe, D. A.; Kleinman, L.; Sedlacek, A. J.; Briggs, N. L.; Hee, J.; Fortner, E.; Shilling, J. E.; Worsnop, D.; Yokelson, R. J.; Parworth, C.; Ge, X. L.; Xu, J. Z.; Butterfield, Z.; Chand, D.; Dubey, M. K.; Pekour, M. S.; Springston, S.; Zhang, Q. Regional influence of aerosol emissions from wildfires

DOI: 10.1021/acsearthspacechem.9b00125
ACS Earth Space Chem. 2019, 3, 1237−1247

driven by combustion efficiency: Insights from the BBOP campaign. *Environ. Sci. Technol.* **2016**, *50* (16), 8613−8622.
(15) May, A. A.; Lee, T.; McMeeking, G. R.; Akagi, S.; Sullivan, A. P.; Urbanski, S.; Yokelson, R. J.; Kreidenweis, S. M. Observations and analysis of organic aerosol evolution in some prescribed fire smoke plumes. *Atmos. Chem. Phys.* **2015**, *15* (11), 6323−6335.
(16) May, A. A.; McMeeking, G. R.; Lee, T.; Taylor, J. W.; Craven, J. S.; Burling, I.; Sullivan, A. P.; Akagi, S.; Collett, J. L.; Flynn, M.; Coe, H.; Urbanski, S. P.; Seinfeld, J. H.; Yokelson, R. J.; Kreidenweis, S. M. Aerosol emissions from prescribed fires in the United States: A synthesis of laboratory and aircraft measurements. *J. Geophys Res-Atmos* **2014**, *119* (20), 11826−11849.
(17) Jolleys, M. D.; Coe, H.; McFiggans, G.; McMeeking, G. R.; Lee, T.; Kreidenweis, S. M.; Collett, J. L.; Sullivan, A. P. Organic aerosol emission ratios from the laboratory combustion of biomass fuels. *J. Geophys Res-Atmos* **2014**, *119* (22), 12850−12871.
(18) Jen, C. N.; Hatch, L. E.; Selimovic, V.; Yokelson, R. J.; Weber, R.; Fernandez, A. E.; Kreisberg, N. M.; Barsanti, K. C.; Goldstein, A. H. Speciated and total emission factors of particulate organics from burning western US wildland fuels and their dependence on combustion efficiency. *Atmos. Chem. Phys.* **2019**, *19* (2), 1013−1026.
(19) Ahern, A. T.; Robinson, E. S.; Tkacik, D. S.; Saleh, R.; Hatch, L. E.; Barsanti, K. C.; Stockwell, C. E.; Yokelson, R. J.; Presto, A. A.; Robinson, A. L.; Sullivan, R. C.; Donahue, N. M. Production of secondary organic aerosol during aging of biomass-burning smoke from fresh fuels and its relationship to VOC precursors. *J. Geophys. Res.: Atmos.* **2019**, *124*, 3583−3606.
(20) May, A. A.; Levin, E. J. T.; Hennigan, C. J.; Riipinen, I.; Lee, T.; Collett, J. L.; Jimenez, J. L.; Kreidenweis, S. M.; Robinson, A. L. Gas-particle partitioning of primary organic aerosol emissions: 3. Biomass burning. *J. Geophys Res-Atmos* **2013**, *118* (19), 11327−11338.
(21) Donahue, N. M.; Robinson, A. L.; Pandis, S. N. Atmospheric organic particulate matter: From smoke to secondary organic aerosol. *Atmos. Environ.* **2009**, *43* (1), 94−106.
(22) Jolleys, M. D.; Coe, H.; McFiggans, G.; Taylor, J. W.; O'Shea, S. J.; Le Breton, M.; Bauguitte, S. J. B.; Moller, S.; Di Carlo, P.; Aruffo, E.; Palmer, P. I.; Lee, J. D.; Percival, C. J.; Gallagher, M. W. Properties and evolution of biomass burning organic aerosol from Canadian boreal forest fires. *Atmos Chem. Phys.* **2015**, *15* (6), 3077−3095.
(23) Cubison, M. J.; Ortega, A. M.; Hayes, P. L.; Farmer, D. K.; Day, D.; Lechner, M. J.; Brune, W. H.; Apel, E.; Diskin, G. S.; Fisher, J. A.; Fuelberg, H. E.; Hecobian, A.; Knapp, D. J.; Mikoviny, T.; Riemer, D.; Sachse, G. W.; Sessions, W.; Weber, R. J.; Weinheimer, A. J.; Wisthaler, A.; Jimenez, J. L. Effects of aging on organic aerosol from open biomass burning smoke in aircraft and laboratory studies. *Atmos. Chem. Phys.* **2011**, *11* (23), 12049−12064.
(24) Akagi, S. K.; Craven, J. S.; Taylor, J. W.; McMeeking, G. R.; Yokelson, R. J.; Burling, I. R.; Urbanski, S. P.; Wold, C. E.; Seinfeld, J. H.; Coe, H.; Alvarado, M. J.; Weise, D. R. Evolution of trace gases and particles emitted by a chaparral fire in California. *Atmos. Chem. Phys.* **2012**, *12* (3), 1397−1421.
(25) Hobbs, P. V.; Sinha, P.; Yokelson, R. J.; Christian, T. J.; Blake, D. R.; Gao, S.; Kirchstetter, T. W.; Novakov, T.; Pilewskie, P. Evolution of gases and particles from a savanna fire in South Africa. *J. Geophys Res-Atmos* **2003**, *108* (D13), 8485.
(26) Liu, X. X.; Zhang, Y.; Huey, L. G.; Yokelson, R. J.; Wang, Y.; Jimenez, J. L.; Campuzano-Jost, P.; Beyersdorf, A. J.; Blake, D. R.; Choi, Y.; St. Clair, J. M.; Crounse, J. D.; Day, D. A.; Diskin, G. S.; Fried, A.; Hall, S. R.; Hanisco, T. F.; King, L. E.; Meinardi, S.; Mikoviny, T.; Palm, B. B.; Peischl, J.; Perring, A. E.; Pollack, I. B.; Ryerson, T. B.; Sachse, G.; Schwarz, J. P.; Simpson, I. J.; Tanner, D. J.; Thornhill, K. L.; Ullmann, K.; Weber, R. J.; Wennberg, P. O.; Wisthaler, A.; Wolfe, G. M.; Ziemba, L. D. Agricultural fires in the southeastern US during SEAC(4)RS: Emissions of trace gases and particles and evolution of ozone, reactive nitrogen, and organic aerosol. *J. Geophys Res-Atmos* **2016**, *121* (12), 7383−7414.
(27) Jimenez, J. L.; Canagaratna, M. R.; Donahue, N. M.; Prevot, A. S. H.; Zhang, Q.; Kroll, J. H.; DeCarlo, P. F.; Allan, J. D.; Coe, H.; Ng, N. L.; Aiken, A. C.; Docherty, K. S.; Ulbrich, I. M.; Grieshop, A. P.; Robinson, A. L.; Duplissy, J.; Smith, J. D.; Wilson, K. R.; Lanz, V. A.; Hueglin, C.; Sun, Y. L.; Tian, J.; Laaksonen, A.; Raatikainen, T.; Rautiainen, J.; Vaattovaara, P.; Ehn, M.; Kulmala, M.; Tomlinson, J. M.; Collins, D. R.; Cubison, M. J.; Dunlea, E. J.; Huffman, J. A.; Onasch, T. B.; Alfarra, M. R.; Williams, P. I.; Bower, K.; Kondo, Y.; Schneider, J.; Drewnick, F.; Borrmann, S.; Weimer, S.; Demerjian, K.; Salcedo, D.; Cottrell, L.; Griffin, R.; Takami, A.; Miyoshi, T.; Hatakeyama, S.; Shimono, A.; Sun, J. Y.; Zhang, Y. M.; Dzepina, K.; Kimmel, J. R.; Sueper, D.; Jayne, J. T.; Herndon, S. C.; Trimborn, A. M.; Williams, L. R.; Wood, E. C.; Middlebrook, A. M.; Kolb, C. E.; Baltensperger, U.; Worsnop, D. R. Evolution of organic aerosols in the atmosphere. *Science* **2009**, *326* (5959), 1525−1529.
(28) Trentmann, J.; Andreae, M. O.; Graf, H. F. Chemical processes in a young biomass-burning plume. *J. Geophys. Res.* **2003**, *108* (D22), 4705.
(29) Hennigan, C. J.; Sullivan, A. P.; Collett, J. L.; Robinson, A. L. Levoglucosan stability in biomass burning particles exposed to hydroxyl radicals. *Geophys. Res. Lett.* **2010**, *37*, L09806.
(30) Jaffe, D. A.; Wigder, N. L. Ozone production from wildfires: A critical review. *Atmos. Environ.* **2012**, *51*, 1−10.
(31) DeCarlo, P. F.; Kimmel, J. R.; Trimborn, A.; Northway, M. J.; Jayne, J. T.; Aiken, A. C.; Gonin, M.; Fuhrer, K.; Horvath, T.; Docherty, K. S.; Worsnop, D. R.; Jimenez, J. L. Field-deployable, high-resolution, time-of-flight aerosol mass spectrometer. *Anal. Chem.* **2006**, *78* (24), 8281−8289.
(32) Bahreini, R.; Dunlea, E. J.; Matthew, B. M.; Simons, C.; Docherty, K. S.; DeCarlo, P. F.; Jimenez, J. L.; Brock, C. A.; Middlebrook, A. M. Design and operation of a pressure-controlled inlet for airborne sampling with an aerodynamic aerosol lens. *Aerosol Sci. Technol.* **2008**, *42* (6), 465−471.
(33) Ortega, A. M.; Day, D. A.; Cubison, M. J.; Brune, W. H.; Bon, D.; de Gouw, J. A.; Jimenez, J. L. Secondary organic aerosol formation and primary organic aerosol oxidation from biomass-burning smoke in a flow reactor during FLAME-3. *Atmos. Chem. Phys.* **2013**, *13* (22), 11551−11571.
(34) Schwarz, J. P.; Gao, R. S.; Fahey, D. W.; Thomson, D. S.; Watts, L. A.; Wilson, J. C.; Reeves, J. M.; Darbeheshti, M.; Baumgardner, D. G.; Kok, G. L.; Chung, S. H.; Schulz, M.; Hendricks, J.; Lauer, A.; Karcher, B.; Slowik, J. G.; Rosenlof, K. H.; Thompson, T. L.; Langford, A. O.; Loewenstein, M.; Aikin, K. C. Single-particle measurements of midlatitude black carbon and light-scattering aerosols from the boundary layer to the lower stratosphere. *J. Geophys. Res.* **2006**, *111*, D16207.
(35) Stephens, M.; Turner, N.; Sandberg, J. Particle identification by laser-induced incandescence in a solid-state laser cavity. *Appl. Opt.* **2003**, *42* (19), 3726−3736.
(36) Lebegue, B.; Schmidt, M.; Ramonet, M.; Wastine, B.; Kwok, C. Y.; Laurent, O.; Belviso, S.; Guemri, A.; Philippon, C.; Smith, J.; Conil, S. Comparison of nitrous oxide (N2O) analyzers for high-precision measurements of atmospheric mole fractions. *Atmos. Meas. Tech.* **2016**, *9* (3), 1221−1238.
(37) Yokelson, R. J.; Andreae, M. O.; Akagi, S. K. Pitfalls with the use of enhancement ratios or normalized excess mixing ratios measured in plumes to characterize pollution sources and aging. *Atmos. Meas. Tech.* **2013**, *6* (8), 2155−2158.
(38) Seinfeld, J. H.; Pandis, S. N. *Atmospheric Chemistry and Physics: From Air Pollution to Climate Change*; John Wiley: Hoboken, NJ, 2006.
(39) Griffin, R. J.; Chen, J. J.; Carmody, K.; Vutukuru, S.; Dabdub, D. Contribution of gas phase oxidation of volatile organic compounds to atmospheric carbon monoxide levels in two areas of the United States. *J. Geophys. Res.* **2007**, *112*, D10S17.
(40) Akagi, S. K.; Yokelson, R. J.; Burling, I. R.; Meinardi, S.; Simpson, I.; Blake, D. R.; McMeeking, G. R.; Sullivan, A.; Lee, T.; Kreidenweis, S.; Urbanski, S.; Reardon, J.; Griffith, D. W. T.; Johnson, T. J.; Weise, D. R. Measurements of reactive trace gases and variable O3 formation rates in some South Carolina biomass burning plumes. *Atmos. Chem. Phys.* **2013**, *13* (3), 1141−1165.

DOI: 10.1021/acsearthspacechem.9b00125
ACS Earth Space Chem. 2019, 3, 1237−1247

(41) Lareau, N. P.; Clements, C. B. The mean and turbulent properties of a wildfire convective plume. *J. Appl. Meteorol Clim* **2017**, *56* (8), 2289−2299.
(42) Bian, Q. J.; Jathar, S. H.; Kodros, J. K.; Barsanti, K. C.; Hatch, L. E.; May, A. A.; Kreidenweis, S. M.; Pierce, J. R. Secondary organic aerosol formation in biomass-burning plumes: theoretical analysis of lab studies and ambient plumes. *Atmos. Chem. Phys.* **2017**, *17* (8), 5459−5475.
(43) Aiken, A. C.; Decarlo, P. F.; Kroll, J. H.; Worsnop, D. R.; Huffman, J. A.; Docherty, K. S.; Ulbrich, I. M.; Mohr, C.; Kimmel, J. R.; Sueper, D.; Sun, Y.; Zhang, Q.; Trimborn, A.; Northway, M.; Ziemann, P. J.; Canagaratna, M. R.; Onasch, T. B.; Alfarra, M. R.; Prevot, A. S. H.; Dommen, J.; Duplissy, J.; Metzger, A.; Baltensperger, U.; Jimenez, J. L. O/C and OM/OC ratios of primary, secondary, and ambient organic aerosols with high-resolution time-of-flight aerosol mass spectrometry. *Environ. Sci. Technol.* **2008**, *42* (12), 4478−4485.
(44) Canagaratna, M. R.; Jimenez, J. L.; Kroll, J. H.; Chen, Q.; Kessler, S. H.; Massoli, P.; Hildebrandt Ruiz, L.; Fortner, E.; Williams, L. R.; Wilson, K. R.; Surratt, J. D.; Donahue, N. M.; Jayne, J. T.; Worsnop, D. R. Elemental ratio measurements of organic compounds using aerosol mass spectrometry: characterization, improved calibration, and implications. *Atmos. Chem. Phys.* **2015**, *15* (1), 253−272.
(45) Simoneit, B. R. T.; Schauer, J. J.; Nolte, C. G.; Oros, D. R.; Elias, V. O.; Fraser, M. P.; Rogge, W. F.; Cass, G. R. Levoglucosan, a tracer for cellulose in biomass burning and atmospheric particles. *Atmos. Environ.* **1999**, *33* (2), 173−182.
(46) Schneider, J.; Weimer, S.; Drewnick, F.; Borrmann, S.; Helas, G.; Gwaze, P.; Schmid, O.; Andreae, M. O.; Kirchner, U. Mass spectrometric analysis and aerodynamic properties of various types of combustion-related aerosol particles. *Int. J. Mass Spectrom.* **2006**, *258* (1−3), 37−49.
(47) Lee, T.; Sullivan, A. P.; Mack, L.; Jimenez, J. L.; Kreidenweis, S. M.; Onasch, T. B.; Worsnop, D. R.; Malm, W.; Wold, C. E.; Hao, W. M.; Collett, J. L. Chemical smoke marker emissions during flaming and smoldering phases of laboratory open burning of wildland fuels. *Aerosol Sci. Technol.* **2010**, *44* (9), I−V.
(48) Cappa, C. D.; Jimenez, J. L. Quantitative estimates of the volatility of ambient organic aerosol. *Atmos. Chem. Phys.* **2010**, *10* (12), 5409−5424.
(49) Shrivastava, M. K.; Lipsky, E. M.; Stanier, C. O.; Robinson, A. L. Modeling semivolatile organic aerosol mass emissions from combustion systems. *Environ. Sci. Technol.* **2006**, *40* (8), 2671−2677.
(50) Hoffmann, D.; Tilgner, A.; Iinuma, Y.; Herrmann, H. Atmospheric stability of levoglucosan: A detailed laboratory and modeling study. *Environ. Sci. Technol.* **2010**, *44* (2), 694−699.
(51) Kuwata, M.; Zorn, S. R.; Martin, S. T. Using elemental ratios to predict the density of organic material composed of carbon, hydrogen, and oxygen. *Environ. Sci. Technol.* **2012**, *46* (2), 787−794.
(52) Salcedo, D.; Onasch, T. B.; Dzepina, K.; Canagaratna, M. R.; Zhang, Q.; Huffman, J. A.; DeCarlo, P. F.; Jayne, J. T.; Mortimer, P.; Worsnop, D. R.; Kolb, C. E.; Johnson, K. S.; Zuberi, B.; Marr, L. C.; Volkamer, R.; Molina, L. T.; Molina, M. J.; Cardenas, B.; Bernabe, R. M.; Marquez, C.; Gaffney, J. S.; Marley, N. A.; Laskin, A.; Shutthanandan, V.; Xie, Y.; Brune, W.; Lesher, R.; Shirley, T.; Jimenez, J. L. Characterization of ambient aerosols in Mexico City during the MCMA-2003 campaign with Aerosol Mass Spectrometry: results from the CENICA Supersite. *Atmos. Chem. Phys.* **2006**, *6*, 925−946.
(53) Duplissy, J.; DeCarlo, P. F.; Dommen, J.; Alfarra, M. R.; Metzger, A.; Barmpadimos, I.; Prevot, A. S. H.; Weingartner, E.; Tritscher, T.; Gysel, M.; Aiken, A. C.; Jimenez, J. L.; Canagaratna, M. R.; Worsnop, D. R.; Collins, D. R.; Tomlinson, J.; Baltensperger, U. Relating hygroscopicity and composition of organic aerosol particulate matter. *Atmos. Chem. Phys.* **2011**, *11* (3), 1155−1165.
(54) Lambe, A. T.; Cappa, C. D.; Massoli, P.; Onasch, T. B.; Forestieri, S. D.; Martin, A. T.; Cummings, M. J.; Croasdale, D. R.; Brune, W. H.; Worsnop, D. R.; Davidovits, P. Relationship between oxidation level and optical properties of secondary organic aerosol. *Environ. Sci. Technol.* **2013**, *47* (12), 6349−6357.

DOI: 10.1021/acsearthspacechem.9b00125
ACS Earth Space Chem. 2019, 3, 1237−1247